



Kineto-static analysis of an articulated six-wheel rover

Philippe Bidaud, Faiz Ben Amar, Tarik Poulain

► To cite this version:

Philippe Bidaud, Faiz Ben Amar, Tarik Poulain. Kineto-static analysis of an articulated six-wheel rover. 8th International Conference on Climbing and Walking Robots and the Support Technologies for Mobile Machines (CLAWAR 2005), Sep 2005, Londres, United Kingdom. pp.475-484, 10.1007/3-540-26415-9_57 . hal-03178084

HAL Id: hal-03178084

<https://hal.science/hal-03178084>

Submitted on 24 Mar 2021

HAL is a multi-disciplinary open access archive for the deposit and dissemination of scientific research documents, whether they are published or not. The documents may come from teaching and research institutions in France or abroad, or from public or private research centers.

L'archive ouverte pluridisciplinaire **HAL**, est destinée au dépôt et à la diffusion de documents scientifiques de niveau recherche, publiés ou non, émanant des établissements d'enseignement et de recherche français ou étrangers, des laboratoires publics ou privés.

Kineto-static analysis of an articulated six-wheel rover

Philippe Bidaud, Faiz Benamar, and Tarik Poulain

Laboratoire de Robotique de Paris - Université Paris 6 / CNRS
18, route du Panorama - 92265 Fontenay Aux Roses - France
bidaud@robot.jussieu.fr

Abstract

In this paper, a kineto-static analysis for an articulated six-wheeled rover called RobuRoc is investigated. A methodology based on reciprocal screw systems is developed for the kinematic modeling and analysis of such multi-monocycle like kinematic structure. A six dimensional force ellipsoid is introduced for the evaluation of traction performances.

1 Introduction

RobuRoc (shown in **Fig.1**) has been designed and built by RoboSoft [1] in response to a Research Program launched in 2004 by the French Defense Agency (DGA - Délégation Générale l'Armement) called MiniRoc whose aim is to develop and evaluate experimentally several semi-autonomous system serving as an extensions of the human soldier. RobuRoc belongs to this class of robot vehicle named Tactical Mobile Robot (TMR). TMRs are basically high mobility small vehicles supposed to operate in highly uncertain urban environments including outdoors and indoors as well. TMR development did not truly begin until the early 1990s. Until then, the military's primary focus for ground robotics was in developing Unmanned Ground Vehicles (UGVs). Nevertheless, various families of TMRs have been developed during the last decade [2]. Their design is more compact and robust than exploration robotics vehicles and have to satisfy specific operational requirements (see [3]).

One of the features of RobuRoc is its ability to operate in extremely rough terrain and negotiating stairs or clear obstacles with height greater

than its wheel radius. Moreover, the vehicle concept was designed to offer reconfiguration capabilities for providing either a maximum of ground adaptation for traction optimization or a high manoeuvrability. RobuRoc kinematics can be seen as a series of 3 unicycle modules linked together by two orthogonal rotoid passive joints. It has been optimized for stair-climbing as well as several typical bumps and jumps clearance.

The paper introduces a methodology for the kinematic modeling and analysis of such locomotion system. An equivalent kinematic model which encapsulate monocycle sub-system kinematics is proposed. The mobility of the whole mechanism is then analyzed using the theory of reciprocal screws. From the kinematic model the concept of traction ellipsoid is introduced for evaluating quantitatively the obstacle clearance capabilities when the configuration of the system and the contact conditions are changing.

2 Kinematic modeling and analysis

2.1 Mobility requirements

The RobuRoc is an articulated wheeled robot vehicle designed for use in urban environments. Urban environments typically include open spaces such as city streets and building interiors. Common obstacles that robots encounter in urban environments include : curbs, stairs, small rubble piles, pipes, railroad tracks, furniture, and wires. The ability to surmount these obstacles is essential for the success of their missions.

2.2 Kinematic description

RobuRoc has a multi-monocycle like kinematic structure as depicted in **Fig.1**. It consists of three pods steered and driven by 2 actuated conventional wheels on which a lateral slippage may occur. The rear and the front pods are symmetrically arranged about the central pod. They are attached to this later one by 2 orthogonal passive rotoid joints providing a roll/pitch relative motion for keeping the wheels on the ground to maintain traction of the pod when traversing irregular surfaces.

2.3 Kinematic modeling

Kinematics plays a fundamental role in design, dynamic modeling, and control. In this section, we illustrate a methodology for modeling and

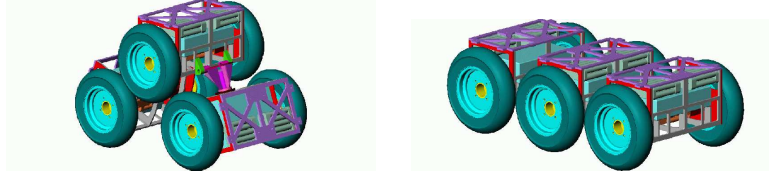


Fig. 1. MiniRoc in a 4 wheels (left) and 6 wheels (right) configurations

analysis of articulated multi-monocycle mobile robots. The obtention of the relationship between the central-pod velocity in a reference frame and wheel velocity vector can be greatly facilitated by extending the methodology used for parallel mechanisms [4] to articulated multi-monocycle asymmetric mechanisms. A parallel manipulator typically consists of several limbs, made up of an open loop mechanism, connecting a moving platform to the ground. Here, the body S_0 of central module can be seen as the moving platform. It is connected to the ground by a differential steering system as well as by the rear and the front modules which can be seen as 2 others "limbs" connecting the S_0 to the ground.

Jacobian of a module: Each individual module j ($j = 0$ for the central, $j = 1, 2$ for the others) can be modeled as an equivalent serial open-chain mechanism (see **Fig.2**).

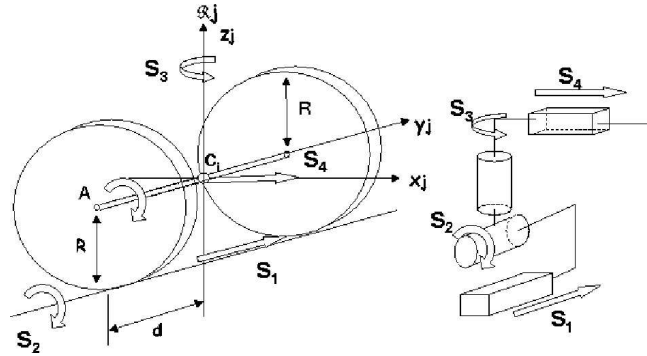


Fig. 2. The differential driving wheels mechanism (left) and its equivalent open-chain mechanism (right)

The differential driving wheels mechanism kinematics can be represented in the \mathcal{R}_i local frame by a set of four unit instantaneous twists

$\hat{\$}_j = (s_i, s_{0i}^* = p_0 \wedge s_i + \mu_i s_i)^t$ $i = 1, 4$ where s_i is a unit vector along the direction of the screw axis, p_0 is the position vector of any point of the screw axis with respect to the origin O of a reference frame and μ_i is the pitch of the screw. The scalar coordinates of these screws written at the axle middle point C_j are:

$$\hat{\$}_1 = [0, 0, 0, 0, 1, 0]^t \quad \hat{\$}_2 = [0, 1, 0, R, 0, 0]^t \quad \hat{\$}_3 = [0, 0, 1, 0, 0, 0]^t \quad \hat{\$}_4 = [0, 0, 0, 1, 0, 0]^t$$

The orthogonal complement in the screw space of the system $\{\hat{\$}_1, \hat{\$}_2, \hat{\$}_3, \hat{\$}_4\}$ has a dimension 2. It represents the pod motions which are not feasible due to the wheel/soil constraints. For the module j , the amplitude ω_{z_j} and v_{x_j} of the screws $\hat{\$}_3^j$ and $\hat{\$}_4^j$ are related to left and the right differentially driven wheels velocities $(\dot{\theta}_{j1}, \dot{\theta}_{j2})$ by the relationship:

$$\begin{pmatrix} \omega_{z_j} \\ v_{x_j} \end{pmatrix} = 1/2 \begin{pmatrix} R/d & -R/d \\ R & R \end{pmatrix} \begin{pmatrix} \dot{\theta}_{1_j} \\ \dot{\theta}_{2_j} \end{pmatrix}$$

or in a compact matrix form:

$$\dot{q}_j = J_{a_j} \dot{\theta}_j \quad (1)$$

where R is the radius of the wheels and d is half length of the width of unicycle module. J_{a_j} is Jacobian matrix of the active part of the pod mechanism.

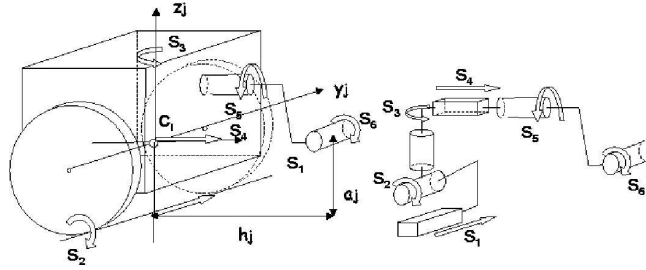


Fig. 3. The differential driving wheels mechanism (left) and its equivalent open-chain mechanism (right) (front/rear module)

Reciprocal Screws of the 3 limbs By referring to the notation introduced in **Fig.3**, the instantaneous twist $\$P$ of the central body can be expressed

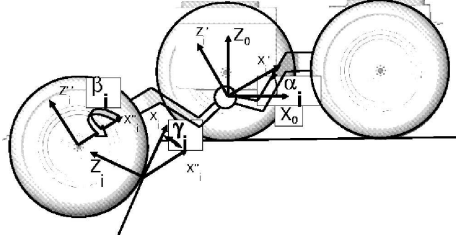


Fig. 4. Definition of α_j , β_j and γ_j angles.

as a linear combination of the n actuated and non-actuated joints screws of each j sub-chain:

$$\$_P = \sum_{i=1}^n \dot{q}_i^j \hat{\$_i^j}$$

where \dot{q}_i^j and $\hat{\$_i^j}$ denote the intensity and the unit screw associated with the i th joint of the j th limb. By considering alternatively the $j = 0, 1, 2$ (which denote respectively the labels for the central, front and rear pods), we obtain:

$$\$_P = \dot{q}_1^0 \hat{\$_1^0} + \dot{q}_2^0 \hat{\$_2^0} + \omega_{z_0}^0 \hat{\$_3^0} + v_{x_0}^0 \hat{\$_4^0} \quad (2)$$

$$\$_P = \dot{q}_1^1 \hat{\$_1^1} + \dot{q}_2^1 \hat{\$_2^1} + \omega_{z_1}^1 \hat{\$_3^1} + v_{x_1}^1 \hat{\$_4^1} + \dot{q}_5^1 \hat{\$_5^1} + \dot{q}_6^1 \hat{\$_6^1} \quad (3)$$

$$\$_P = \dot{q}_1^2 \hat{\$_1^2} + \dot{q}_2^2 \hat{\$_2^2} + \omega_{z_2}^2 \hat{\$_3^2} + v_{x_2}^2 \hat{\$_4^2} + \dot{q}_5^2 \hat{\$_5^2} + \dot{q}_6^2 \hat{\$_6^2} \quad (4)$$

Equations (2) (3) (4) contain many unactuated joint rates that must be eliminated to reach a relationship between the instantaneous screw which defines the absolute motion $\$_P$ of the central body and the wheel's velocities vector $\dot{\theta}$. This can be done very efficiently by using a set of reciprocal screws $\hat{\$_i^{rj}}$ associated with all the actuated joints (of order i in the equivalent open chain) of the j th limb. A detailed description of screw systems can be found in [5]. We will only recall that two screws $\hat{\$_1}$ and $\hat{\$_2}$ are said reciprocal if they satisfy the condition:

$$s_1 \cdot s_{02}^* + s_2 \cdot s_{01}^* = 0$$

To simplify the expression, we will consider the particular situation where $\beta_j = 0$ ($j = 1, 2$). The coordinates of screw $\hat{\$_3^{rj}}$ and $\hat{\$_4^{rj}}$ that are reciprocal to all screws except for respectively $\hat{\$_3^j}$ and $\hat{\$_4^j}$ for $j = 1, 2$ expressed at the point 0_0 (origin of \mathcal{R}_j frame) and in the \mathcal{R}_j frame are (see figure 4)⁽¹⁾:

¹ $C \equiv \cos$ and $S \equiv \sin$

$$\hat{\$}_3^j = [0, 0, 0, S\gamma_j, 0, C\gamma_j]^t \text{ for } j=1,2 \quad (5)$$

$$\hat{\$}_4^j = \left[C\lambda_j = \frac{h_j}{\sqrt{a_j^2 + h_j^2}}, 0, S\lambda_j = \frac{a_j}{\sqrt{a_j^2 + h_j^2}}, 0, 0, 0 \right]^t \text{ for } j=1,2 \quad (6)$$

The reciprocal screws $\hat{\$}_3^0$ and $\hat{\$}_4^0$ have to be determined by considering the 4-system $\{\hat{\$}_1^0, \hat{\$}_2^0, \hat{\$}_3^0, \hat{\$}_4^0\}$ of feasible motions. They are $\hat{\$}_3^0 = [0, 0, 1, 0, 0, 0]^t$ and $\hat{\$}_4^0 = [1, 0, 0, 0, a_0, 0]^t$.

These reciprocal screws represent physically the elementary wrenches developed by the module j on the central body resulting from the action f_{x_i} and m_{z_i} of the equivalent active joints 3 and 4 knowing that these actions are related to the wheel joint torques τ_{1_j} and τ_{2_j} by:

$$\begin{pmatrix} m_{z_j} \\ f_{x_j} \end{pmatrix} = 1/2 \begin{pmatrix} d/R & -d/R \\ 1/R & 1/R \end{pmatrix} \begin{pmatrix} \tau_{1_j} \\ \tau_{2_j} \end{pmatrix} = J_a^{-t} \tau_j$$

Their coordinates in the \mathcal{R}_0 frame are directly computed by multiplying (5) and (6) by the block matrix:

$$E_{0j} = \left(\begin{array}{c|c} R_{j0}^t & 0_{3 \times 3} \\ \hline 0_{3 \times 3} & R_{j0}^t \end{array} \right) \quad (7)$$

with the rotation matrix R_{j0} given here for $\beta_j \neq 0$:

$$R_{j0} = \begin{pmatrix} C\alpha_j C\gamma_j - S\alpha_j C\beta_j S\gamma_j & S\beta_j S\gamma_j & -S\alpha_j C\gamma_j - C\alpha_j C\beta_j S\gamma_j \\ S\beta_j S\alpha_j & C\beta_j & S\beta_j C\alpha_j \\ C\alpha_j S\gamma_j + S\alpha_j C\beta_j C\gamma_j & -S\beta_j C\gamma_j & -S\alpha_j S\gamma_j + C\alpha_j C\beta_j C\gamma_j \end{pmatrix}$$

By multiply each side of the equation with the reciprocal screws, it produces a set of equations which can be written in a matrix form as follows:

$$B\dot{q}_a = D\$_P$$

with $\dot{q}_a = (\omega_{z_1}, v_{x_1}, \omega_{z_0}, v_{x_0}, \omega_{z_2}, v_{x_2})^t$, ω_{z_j} and v_{x_j} denoting respectively the linear and angular velocities produced by the differential steering system of the pod j along x_j and about z_j . B is a diagonal matrix whose components are:

$$B = \text{diag}(C\gamma_1, C\lambda_1, 1, 1, C\gamma_2, C\lambda_2) \quad (8)$$

and D is a matrix whose lines are the reciprocal screws coordinates in the frame \mathcal{R}_0 :

$$D = \begin{pmatrix} \hat{\$}_r^1 \\ \hat{\$}_r^3 \\ \hat{\$}_r^1 \\ \hat{\$}_r^4 \\ \hat{\$}_r^0 \\ \hat{\$}_r^3 \\ \hat{\$}_r^0 \\ \hat{\$}_r^4 \\ \hat{\$}_r^2 \\ \hat{\$}_r^3 \\ \hat{\$}_r^2 \end{pmatrix} = \begin{pmatrix} 0 & 0 & 0 & -S\alpha_1 & 0 & C\alpha_1 \\ C\varphi_1 & 0 & S\varphi_1 & 0 & 0 & 0 \\ 0 & 0 & 0 & 0 & 0 & 1 \\ 1 & 0 & 0 & 0 & a_0 & 0 \\ 0 & 0 & 0 & -S\alpha_2 & 0 & C\alpha_2 \\ C\varphi_2 & 0 & S\varphi_2 & 0 & 0 & 0 \end{pmatrix} \quad (9)$$

where $\varphi_j = \lambda_j + \gamma_j + \alpha_j$ when $\beta_j = 0$. If the robot stays on an horizontal plane the angles ($\alpha_j = \beta_j = \gamma_j = 0$) and then the kinematic model reduces to:

$$\begin{pmatrix} 1 & 0 & 0 & 0 & 0 & 0 \\ 0 & C\lambda_1 & 0 & 0 & 0 & 0 \\ 0 & 0 & 1 & 0 & 0 & 0 \\ 0 & 0 & 0 & 1 & 0 & 0 \\ 0 & 0 & 0 & 0 & 1 & 0 \\ 0 & 0 & 0 & 0 & 0 & C\lambda_2 \end{pmatrix} \begin{pmatrix} \omega_{z_1} \\ v_{x_1} \\ \omega_{z_0} \\ v_{x_0} \\ \omega_{z_2} \\ v_{x_2} \end{pmatrix} = \begin{pmatrix} 0 & 0 & 0 & 0 & 0 & 1 \\ C\lambda_1 & 0 & S\lambda_1 & 0 & 0 & 0 \\ 0 & 0 & 0 & 0 & 0 & 1 \\ 1 & 0 & 0 & 0 & a_0 & 0 \\ 0 & 0 & 0 & 0 & 0 & 1 \\ C\lambda_2 & 0 & S\lambda_2 & 0 & 0 & 0 \end{pmatrix} \begin{pmatrix} \bar{v}_{x_0} \\ \bar{v}_{y_0} \\ \bar{v}_{z_0} \\ \bar{\omega}_{x_0} \\ \bar{\omega}_{y_0} \\ \bar{\omega}_{z_0} \end{pmatrix} \quad (10)$$

This model clearly shows that the degree of mobility of the system in this particular case is equal to 4. The lateral velocity of the system is not controlled kinematically as well as the rotation about the x_0 axis. It also tells how a vertical motion (v_{z_0}) of the central pod can be produced. By introducing the block matrix J_a (10):

$$J_a = \left(\begin{array}{c|c|c} J_{a_1} & 0 & 0 \\ \hline 0 & J_{a_0} & 0 \\ \hline 0 & 0 & J_{a_2} \end{array} \right)$$

we obtain the kinematic control model of the vehicle (here for a planar evolution):

$$J_a \dot{\theta} = \begin{pmatrix} 0 & 0 & 0 & 1 \\ 1 & tg\lambda_1 & 0 & 0 \\ 0 & 0 & 0 & 1 \\ 1 & 0 & a_0 & 0 \\ 0 & 0 & 0 & 1 \\ 1 & tg\lambda_2 & 0 & 0 \end{pmatrix} \begin{pmatrix} \bar{v}_{x_0} \\ \bar{v}_{z_0} \\ \bar{\omega}_{y_0} \\ \bar{\omega}_{z_0} \end{pmatrix} = D\dot{X}$$

where $\dot{\theta} = (\dot{\theta}_{11}, \dot{\theta}_{12}, \dot{\theta}_{01}, \dot{\theta}_{02}, \dot{\theta}_{21}, \dot{\theta}_{22})^t$

3 Obstacle clearance capacities and force transmission

A key factor involved in the design of TMR is generating sufficient amounts of force and moment from the actuation system for climbing critical obstacles such as stairs.

The position of the pitch passive joint has been determined to assist the step climbing of the front wheel. From static equilibrium conditions

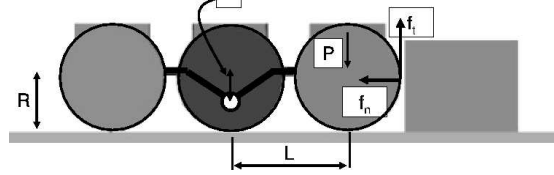


Fig. 5. Pitch passive axis location in the central pod

of the front pod wheels in contact with the front of the step when starting to climb:

$$(L + R)f_t + hf_n = PL \quad (11)$$

When $h > 0$ the normal force component, f_n helps the passive motion of the front wheel about the axis passing through C_0 . **Fig.6** shows sequences of a step clearing using dynamic simulation with Adams software. In this simulation the height of the obstacle is greater than the wheel radius (40cm vs 24cm) and the friction coefficient in wheel-ground contact is 0.6.



Fig. 6. Dynamic simulation with Adams software of a high obstacle clearing.

In the other part, force-moment transmission on the central body is reflecting by the D matrix. Its lines represent the elementary actions (here in the reduced wrench space $(f_{x_0}, f_{z_0}, m_{y_0}, m_{z_0})$) developed by the driving torques $(\tau_{11}, \tau_{12}, \tau_{01}, \tau_{02}, \tau_{21}, \tau_{22})^t$ on the central body. Similarly as when multiple robots exert forces or carry an object in cooperative way, D is equivalent to G^t , G representing the grasp matrix that contains the contact distribution and the way the active forces are transmitted on the

central body. G can be partitioned into 2 blocks $G = (G_f \ G_m)^t$, G_f and G_m representing respectively the force and the moment transmission. It is interesting to be able to compare the traction capabilities for different contact conditions. Hence, the set of forces and moments realizable by τ such $\|\tau\| \leq 1$ form an ellipsoid. A representative measure σ of the traction derived from the image of this unit ball of active joint torques:

$$\sigma = \left[\det(G_f^t G_f) \right]^{1/2} \quad (12)$$

When $\beta_j = 0$ ($j = 1, 2$), the traction index σ is:

$$\sigma = \left[(S\gamma_1 C\gamma_2 - C\gamma_1 S\gamma_2)^2 + S\gamma_1^2 + S\gamma_2^2 \right]^{1/2}$$

This index is equal to zero when G_f is singular. Then the force transmission in the vertical direction becomes null, this happens in configurations where $\gamma_j = 0$ ($j = 1, 2$).

4 Conclusion

This paper presents a general framework for study wheeled modular vehicle composed by monocycles. We show that by using an equivalent kinematic model of a monocycle and the reciprocal screws theory, we derive easily the inverse velocity model that could be used for control and trajectory tracking. The force transmission in these systems is also investigated by making analogy to parallel manipulators and the concept of the manipulability ellipsoid. This theoretical study should be generalized to other vehicle kinematics including those with wheels, legs or with both. Future works should be focused on minimization of torques and energy consumption during manoeuvring or steering along curved trajectory.

5 Acknowledgments

The authors would like to acknowledge DGA/SPART and RoboSoft for offering them the opportunity to develop a scientific activity in the Miniroc framework.

References

1. Robosoft (2005) Robotsoft website. <http://robosoft.fr>.

2. Department of Defense (1989) Dod robotics master plan for unmanned ground vehicles. Conference Report on the Department of Defense Appropriations Act.
3. Pierce, G.M. (2005) Robotics: Military applications for special operations forces. .
4. Mohamed, M.G. and Duffy, J. (1985) A direct determination of the instantaneous kinematics of fully parallel robot manipulators. *ASME Journal*, vol. 107, no. 2.
5. Hunt, K.H. (1978) Kinematic geometry of mechanisms. Clarendon Press.